J. Microelectron. Packag. Soc., 23(2), 57-63 (2016) http://dx.doi.org/10.6117/kmeps.2016.23.2.057
Print ISSN 1226-9360 Online ISSN 2287-7525

Electrospun Magnetic Nanofiber as Multifunctional Flexible EMI-Shielding Layer and its Optimization on the Effectiveness

Jiwoo Yu[1], Dae-Hyun Nam[1], Young-Joo Lee[1] and Young-Chang Joo[1,2,†]

[1]Department of Materials Science and Engineering, Seoul National University, 1 Gwanak-ro, Gwanak-gu, Seoul 151-744, Korea
[2]Research Institute of Advanced Materials (RIAM), Seoul National University, 1 Gwanak-ro, Gwanak-gu, Seoul 151-742, Korea

(Received May 24, 2016: Corrected June 14, 2016: Accepted June 16, 2016)

Abstract: We developed a flexible and micro-thick electromagnetic interference (EMI) shielding nanofabric layer that also functions as a water resisting and heat sinking material. Electrospinning followed by a simple heat treatment process was carried on to produce the EMI-shielding Ni/C hybrid nanofibers. The ambient oxygen partial pressure (pO_2 = 0.1, 0.7, 1.3 Torr) applied during the heat treatment was varied in order to optimize the effectiveness of EMI-shielding by modifying the size and crystallinity of the magnetic Ni nanoparticles distributed throughout the C nanofibers. Permittivity and permeability of the nanofibers under the electromagnetic (EM) wave frequency range of 300 MHz~1 GHz were measured, which implied the EMI-shielding effectiveness (SE) optimization at pO_2 = 0.7 Torr during the heat treatment. The materials' heat diffusivity for both in-plane direction and vertical direction was measured to confirm the anisotropic thermal diffusivity that can effectively deliver and sink the local heat produced during device operations. Also, the nanofibers were aged at room temperature in oxygen ambient for water resisting function.

Keywords: electrospinning, EMI-shielding, magnetic nanofibers, oxygen partial pressure

1. Introduction

As humans in recent years undergo frequent radiofrequency (RF) exposure from electronic devices and local wireless networks, the development of EMI shielding layer that is flexible,[1)] thin, and effective is now in high demand. EM radiation, particularly which at high frequencies that emanate from cellular phones (x-band), is known to irritate and disturb human body signals and, possibly, eventually cause cancer, cataracts, and change in sperm count and motility.[2)] In order to shield EM radiated from emerging flexible devices, an EMI-shielding layer is required to be flexible and free-standing, as the shielding layer is expected to be placed on a stacking of flexible circuits[3-6)] as an additional layer.

The mechanism of EMI shielding is reflection and absorption of EM wave, which shield against the penetration of the EM wave through the shielding layer. For the reflection of the EM radiation, the shield must have mobile charge carriers, electron and holes, which interact with EM fields in the radiation. Therefore, EMI-shielding materials tend to be electrically conductive, although a high conductivity is not a requisite.[7)] The reflection loss is a function of $\sigma/\eta(r)$, where σ is the electrical conductivity relative to copper and $\eta(r)$ is the relative magnetic permeability.[8)]

Absorption is considered to be dominant for shielding EM wave of high frequency. For absorption mechanism, the shield should have electric and/or magnetic dipoles, which as well interact with EM fields in the radiation.[7)] Materials with high permittivity and permeability enhance absorption of EM radiation that occur by dissipation and/or storage of the radiation energy.[9)] The absorption loss is a function of $\sigma \cdot \eta(r)$.[8)]

Multiple reflections, which refer to the reflections at various surfaces or interfaces in the shielding material, require presence of increased surface area. To enhance multiple reflections, metal fillers with size less than ~1 μm has been desired in composites for EMI-shielding. The reduction of particle size to less than ~1 μm does not decrease the SE of the individual particles by skin-effect, therefore, only increases surface area that increases overall SE. By skin-effect, when penetrating a conductor, the EM field of plane wave drops exponentially with increasing depth into the conductor. Therefore, small particles can effectively shield

†Corresponding author
E-mail: ycjoo@snu.ac.kr

EM field as much as larger particles do. However, if the particles are extremely small so that the size is less than skin depth of the material, the particle size effect on individual particle's SE exists, and smaller particles shield smaller amount of EM field. For bulk nickel, assuming permeability of 100 and conductivity of $1.15 \times 10^7\ \Omega^{-1}m^{-1}$, the skin depth is calculated to be 0.47 μm at 1 GHz, which is far larger than the size of the fabricated particles in this study, 4~50 nm.

The total shielding effectiveness of a material, SE_{total}, can be calculated as following:

$$SE_{total}(dB) = SE_A + SE_R + SE_M = 20d\left(\frac{\mu(r)\sigma\omega}{2}\right)^{1/2} \log_{10}(e) + 10\log_{10}\left(\frac{\sigma}{16\mu(r)\omega\varepsilon(0)}\right) + SE_M$$
$$\sigma = 2\pi f\varepsilon'',\ \omega = 2\pi f \quad (1)^{7)}$$

where, SE_A, SE_R, SE_M are shielding effectiveness of absorption, reflections, and multiples reflections, respectively, d is sample thickness, e is 2.718, $\sigma = 2\pi f\varepsilon''$ is electrical conductivity (S/m), $\omega = 2\pi f$ is angular frequency, f is frequency of wave, ε'' is imaginary part of permittivity, $\varepsilon(0)$ is dielectric constant of vacuum.

Conventional EMI-shielding material is micro-thin metal layer formed by spray coating, electroplating, electroless plating, or vacuum depositions. Metal coating by nanoparticle ink spray, shown in Fig. 1(a), has been most commonly used because of its processability and the low cost. However, when applied to flexible electronic devices, where metal ink must be sprayed on a flexible layer such as a polymeric layer, sprayed metal coating is no longer suitable due to concern about poor wear and delamination.[7)]

In replacement of metal coating, there has been emerging research on polymer/metal nanoparticle composite layers for flexible EMI-shielding materials, as shown in Fig. 1(a).[10,11)] However, nanoparticles with high specific surface energy agglomerates in polymer, and the dispersion of the nanoparticles has been the main difficulty. Also, filler-matrix bonding has to be considered to prevent the decrease in strength and ductility of the composite. There has been effort to solve above mentioned problems by simply removing the fillers and using conductive polymers,[12-14)] however, conductive polymers are not common and tend to be poor in processability and mechanical properties.[7)]

To enhance the EMI shielding effectiveness (SE) and flexibility, the magnetic metal nanoparticles dispersed evenly in carbon conducting path is considered to be one of the best forms of EMI shielding material, which we targeted for. We have developed a novel fabrication method, which is simple and cost effective, to control the size and crystallinity of transition metals inside carbon fibers through oxygen partial pressure (pO_2) controlled calcination, for optimizing the effectiveness. Amongst common magnetic metals, Ni was applied due to its superior oxidation resistance, high permeability, and good processability that comes from nickel acetate's excellent solubility with other substances in the solutions prepared for electrospinning.

In addition to the EM radiation shielding, the industry is also facing the increasing demand in heat sink that distribute local heat produced when operating electronic devices.[15,16)] Also, another important needs in the industry is waterproof because not only water directly shorts circuits but also the humidity damage layer adhesions.[17)] The water seeping through microphones and speaker of a mobile phone is a great concern to be solved. The greatest advantages of our material not only lies on its optimized EMI-shielding effectiveness but also on its enhanced anisotropic thermal conductivity and hydrophobicity for its application to multifunctional EMI-shielding layer. We achieved anisotropic

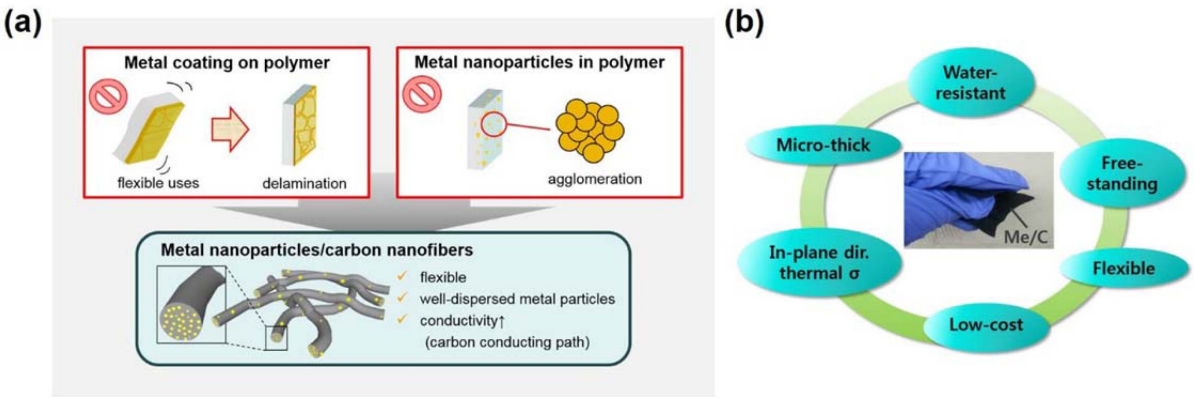

Fig. 1. (a) schematic illustrations on conventional flexible EMI-shielding layers and their limitations. (b) illustration on electrospun nanofiber being an advanced flexible and multifunctional EMI-shielding layer

thermal conductivity in the plane direction for heat sink, and at the same time, dramatically enhanced surface hydrophobicity for water resistance, as shown in Fig. 1(b).

2. Experimental

In order to fabricate Ni/C hybrid nanofibers, we first prepared a solution for electrospinning. Polyacrylonitrile (PAN, M_w=150,000 g/mol, Sigma-Aldrich) and nickel acetate-tetrahydrate (NiAc, M_w=248.84 g/mol, Sigma-Aldrich) were dissolved in dimethylformamide (DMF, M_w=73.09 g/mol, Sigma-Aldrich) by 7 wt.% and 5 wt.%, respectively. After stirring the solution for 4 hours, the solution was loaded into a syringe with a metal needle tip (18G) and was electrospun at a rate of 0.4 mL/h by the potential difference of 15 kV. The electrospun nanofibers were collected and heat-treated under pO_2 (=0.1, 0.7, 1.3 Torr) at 700ºC for 3 hours.

The morphology of the nanofibers was observed using field emission scanning electron microscopy (FE-SEM, Hitachi, SU70) and transmission electron microscopy (TEM, Tecnai, F20). The static magnetic properties of nanofibers at room temperature in the range of from −10000 Oe to 10000 Oe were determined using vibrating sample magnetometer (VSM, Quantum Design, PPMS-14). RF impedance meter (Agilent, E4991A) were used to measure permeability and permittivity in the EM frequency range of 300 MHz~8 GHz to analyze the EMI-SE. The wave guides used to measure permeability and permittivity are Agilent 16454A and 16453A, respectively. The cal-kit used for calibration was Agilent 16195B. Anisotropic heat diffusivity was confirmed by measuring in-plane and vertical direction diffusivity using thermal diffusivity instrument (Netzsch, LFA 447). Static contact angle measurement were carried on using optical tensiometer (Attension, Theta) to determine surface hydrophobicity.

3. Result and Discussion

A heat treatment process after electrospinning the solution is required to convert PAN into carbon and NiAc into Ni nanoparticles. The as-spun nanofibers were heat treated using a calcination technique named selective oxidation. For the selective oxidation, the nanofibers were heat treated under pO_2 instead of under a typical heat treating ambient, high vacuum or the air. The applied pO_2 provides an oxygen level to partially oxidize carbon but not enough oxygen to oxidize the metal composite, therefore, selectively and partially oxidize only carbon but reduce the metal nanoparticles. Selective oxidation is only possible for the metal species that oxidize at higher pO_2 than carbon does at 700ºC, which includes Ni, Co, Cu, Fe, Ag, Pb, and more.[18] For the conventional heat treatment process at high vacuum, the size and crystallinity of the nanoparticles in nanofibers are unable to be modified. For another conventional heat treatment process in the air, all of the carbons are oxidized to be converted to carbon dioxide, leaving no carbon residue, which results in loss in free-standing ability. Also, if heat treated in the air, the nanoparticles are oxidized, which requires an additional heat treat-

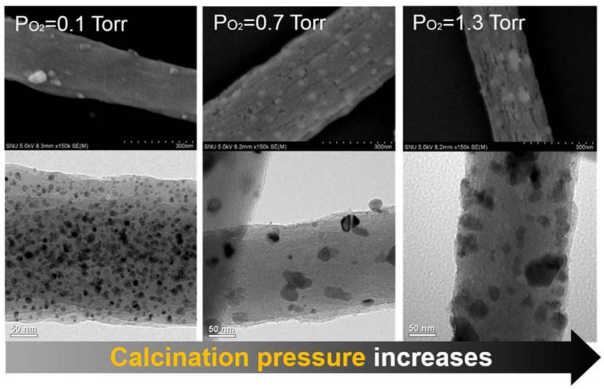

Fig. 2. The morphology modification of Ni/C nanofibers via pO_2 increase during the heat treatment.

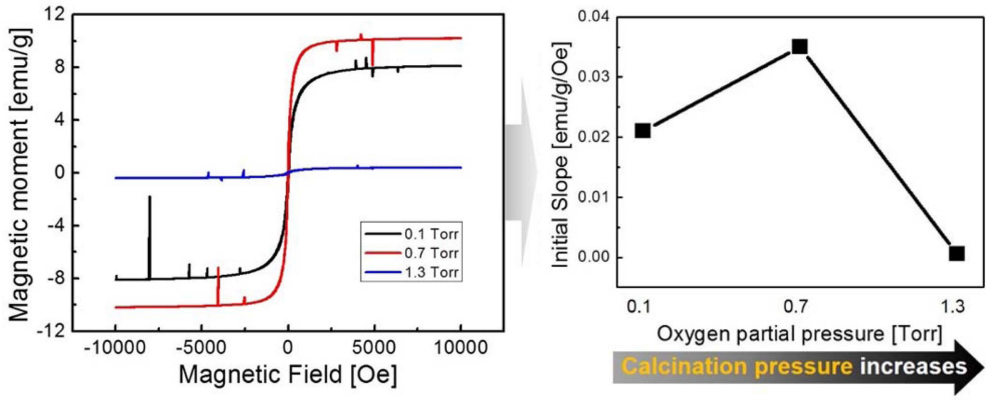

Fig. 3. Magnetic properties of Ni/C nanofibers heat treated in varying oxygen ambient pressure.

ment process in H_2 ambient to convert the metal oxides to metals. For the selective oxidation technique, we used in this study, all the fabricated nanofibers exhibit free-standing ability and the nanoparticles exhibit reduced metal phase.

Morphologies of the nanofibers were observed using FE-SEM and TEM as in Fig. 2. It is obvious that the size of the Ni nanoparticles and the pores of the C nanofibers increased with pO_2 increase during heat treatment. As more pO_2 ambient is applied, the carbon matrix becomes more porous due to combustion, hence the carbon density decreases. With higher pO_2, more carbon has been decomposed, meaning more diffusion barrier for Ni nanoparticles has removed, resulting in enlarged nanoparticle nucleation.

Magnetic properties of the nanofibers were investigated, as shown in Fig. 3, in order to relate it to the permeability for EMI-SE analysis. Permeability is implied in the slope of hysteresis loop, because it represents how well the magnetic spin reacts with external magnetic field applied, which was the highest at pO_2=0.7 Torr. The larger permeability at pO_2=0.7 Torr than at pO_2=0.1 Torr may be attributed to the size increase of magnetic nanoparticles. The magnetic property for the sample heat treated at pO_2=1.3 Torr exhibited the lowest value, which may be attributed to the decrease in crystallinity that increases magnetic domain walls allocated in the nanoparticles.

Figure 4 (a) and (b) shows permittivity and permeability, respectively, of the nanofibers under a EM wave frequency range. The frequency range tested was 0~1 GHz, although the data under f < 300 MHz is unreliable due to the device instability for low frequencies.

For the permittivity and permeability measuring device, impedance meter was used, where a tested nanofiber in size of 3 × 3 cm is placed in between two electrodes, and therefore, surface insulation of tested samples is required. However, since the tested nanofibers are conductive on the surface, paper sheets were placed in between the nanofiber and each electrode, so the measured values are only meaningful for relative comparisons and are not valid for absolute values. Vector network analyzer (VNA) is another common tool for permittivity and permeability measurement over a frequency range, where a tested sample must be perfectly cut in a required shape of about < 5 mm. Nanofibers are hard to be cut sharply in such small shapes. Also, the coaxial line/waveguides connected to the measuring device has to be designed in such a way that they

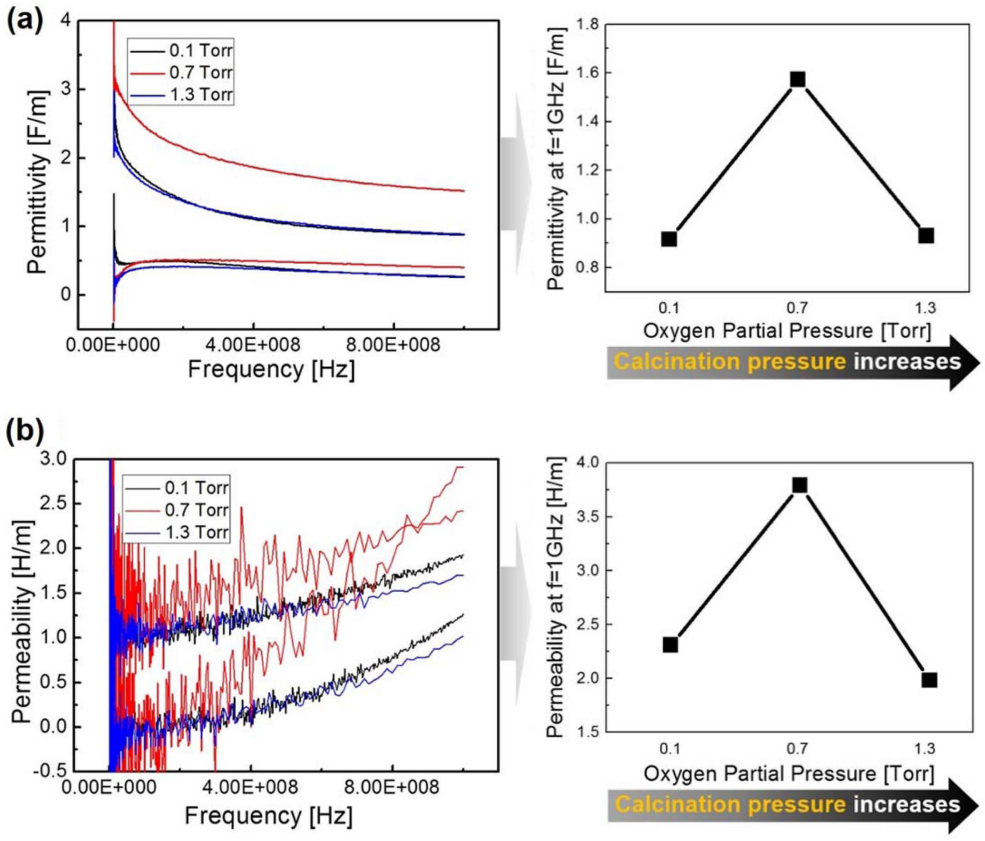

Fig. 4. (a) permittivity and (b) permeability under external EM field of frequency < 1 GHz. The data under the frequency < 300 MHz is considered to be unreliable due to the device instability at low frequencies. The permittivity and permeability at f = 1 GHz for the pO_2 variations are plotted on the right sides of (a) and (b), respectively.

would perfectly deliver EM waves without any loss, which is extremely expensive for obtaining a few measurements. Due to the difficulties, we used impedance meter and were only able to obtain relative values.

In order to compare the samples and analyze the shielding effectiveness, the permittivity and permeability values at the EM wave frequency of 1 GHz were plotted on the right sides of Fig. 4 (a) and (b), respectively. The data at f = 1 GHz was chosen for the analysis because the frequency range emanates from typical mobile phone is about 300 MHz~2 GHz, and 1 GHz is considered to be the closest to the middle of the range. Both permittivity and permeability at f=1 GHz are highest at pO_2=0.7 Torr, aligning with the magnetic property measurement.

SE throughout the EM wave frequency could be calculated, using Equation 1 followed by thickness normalization, if with absolute values for permittivity and permeability. The obtained relative data implies that pO_2=0.7 Torr sample would exhibit the highest SE, known from the following analysis. All the three samples (pO_2=0.1, 0.7, 1.3 Torr) have particles that are much smaller than skin depth, so the particle size would affect the SE of individual particles. Also, the samples are tested in high EM frequency, so absorption mechanism is expected to be dominant over reflections. pO_2=0.1 Torr sample has more reflecting surfaces that would increase SE a bit more but also has the smallest particles of 5nm in average that decreases SE of individual particles. pO_2=0.7 Torr sample is advantageous, compared to the pO_2=0.1 Torr sample, due to larger particles and comparable reflecting surfaces, as well as highest permeability that enables higher absorption. pO_2=1.3 Torr sample has low permeability and less reflection surfaces due to the large size of the particles, therefore, is expected to have the lowest SE_{total}.

The thermal diffusivity of nanofibers for in-plane and out-of-plane directions were measured using thermal diffusivity instrument, and the result is plotted in Fig. 5. Nanofibers heat treated at pO_2=0.1, 0.7, 1.3 Torr showed the heat diffusivity of 20.46, 10.16, 13.74 mm^2/s, respectively for in-plane direction. Thermal conductivity is the product of thermal diffusivity, specific heat capacity, and density, therefore, thermal conductivity of pO_2=0.1 Torr sample with the highest thermal diffusivity and density would still be the highest for in-plane direction. When comparing pO_2=0.7 Torr and pO_2=1.3 Torr samples, the higher density of pO_2=0.7 Torr sample would moderate the lower heat diffusivity, resulting in comparable thermal conductivity for in-plane direction. For vertical direction, the heat diffusivity of nanofibers heat treated at pO_2=0.1, 0.7, 1.3 Torr exhibit 0.323, 0.616, 0.573 mm^2/s, respectively. The anisotropic heat diffusion is very beneficial for heat sink, because the in-plane thermal conductivity distributes local heat produced on neighboring circuit layers during device operation, while the heat insulation in vertical direction prevents heat to be delivered in-between the neighboring circuit layers placed on each sides of the EMI-shielding plane.

The surface hydrophobicity of the nanofibers has been achieved. There are two factors of surface that are known to possibly affect hydrophobicity: morphology and surface energy. Porous, hierarchical, or re-entrant surface morphologies are often used to enhance surface hydrophobicity by supporting water in Cassie-Baxter state.[19] Also, lowering surface energy increases the static contact angle. In our experiment, oxygen aging at room temperature dramatically enhanced the surface hydrophobicity as shown in Fig. 6(a) while it did not change the morphology of the nanofibers. The oxygen aging effect for all the nanofibers were

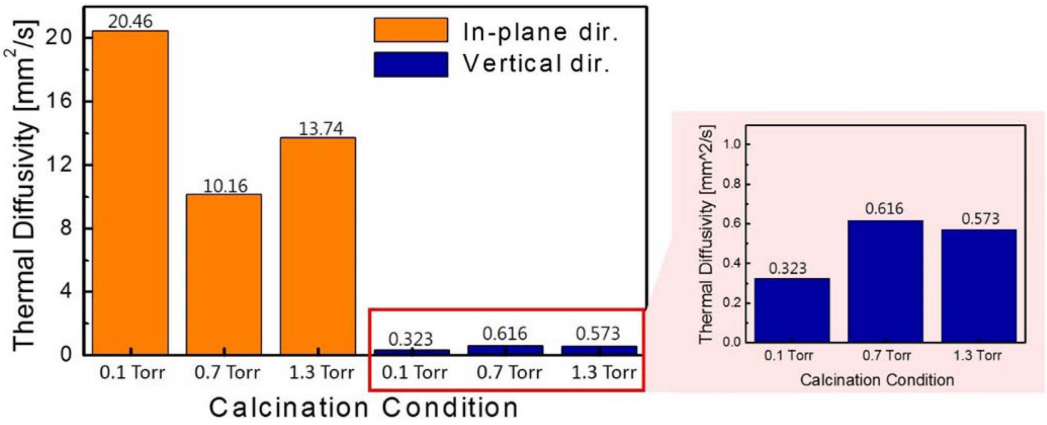

Fig. 5. Thermal diffusivities for pO_2 = 0.1, 0.7, 1.3 Torr samples in plane-direction (orange) and in vertical direction (navy). The thermal diffusivity difference for more than an order of magnitude for in-plane and vertical directions confirms anisotropic thermal conduction, which is ideal for a heat-sinking layer.

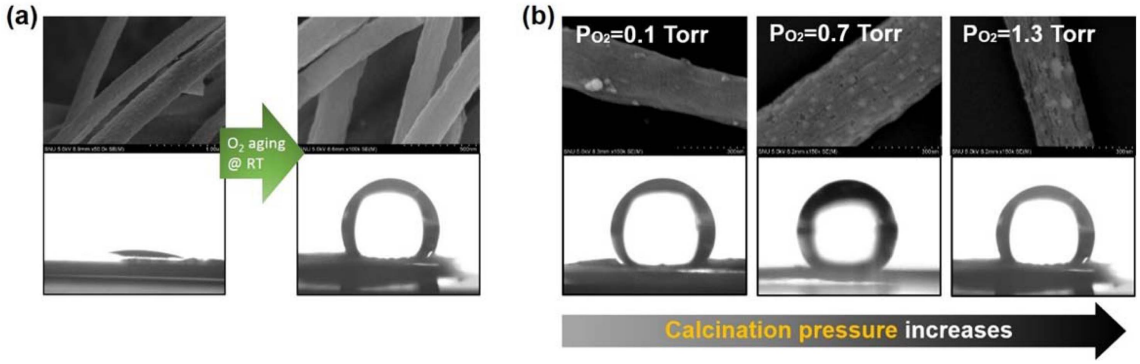

Fig. 6. (a) contact angle measurements for pO_2=1.3 Torr sample before and after oxygen aging at room temperature. (b) contact angle measurements after oxygen aging at room temperature for pO_2=0.1, 0.7, 1.3 Torr samples.

the same, regardless of the morphology or porosity of the nanofibers, as shown in Fig. 6(b). Therefore, it can be said the increase in hydrophobicity is mainly attributed to the surface energy effect rather than morphology effect and the oxygen aging at room temperature decreased the surface energy of the nanofibers. From experience, the oxygen aging at room temperature does not affect the phase or magnetic properties of the nanoparticles, rendering the oxygen aging to be an excellent tool for waterproofing.

4. Conclusion

A micro-thick, flexible, and multifunctional EMI-shielding Ni/C nanofibers were developed with low cost. The nanofibers were successfully modified by applying the ambient pO_2 during heat treatment. The nanofiber modifications optimized permittivity, permeability, hence, EMI-SE. The highest shielding effect achieved at pO_2=0.7 Torr is attributed to the increase in size and crystallinity of the Ni particles in the nanofibers. The fabricated Ni/C nanofibers' heat diffusivity was anisotropic by more than about 30 times in average when comparing in-plane and vertical directions, which can distribute and sink local heat from neighboring circuit layers. In addition, aging treatment in oxygen drastically enhanced surface hydrophobicity, lowering the surface energy of the nanofibers.

Acknowledgement

This research was supported by the MOTIE (Ministry of Trade, Industry & Energy (10051601) and KDRC (Korea Display Research Corporation) support program for the development of future devices technology for display industry. XRD and TEM analysis were supported by the Research Institute of Advanced Materials (RIAM) at Seoul National University. Impedance meter measurements were supported by Gumi Electronics & Information Technology Research Institute (GERI).

References

1. J.-H. Ahn, H. Lee and S.-H. Choa, "Technology of Flexible Semiconductor/Memory Device", J. Microelectron. Packag. Soc., 20(2), 1 (2013).
2. O. Erogul, E. Oztas, I. Yildirim, T. Kir, E. Aydur, G. Komesli, H. C. Irkilata, M. K. Irmak and A. F. Peker, "Effects of electromagnetic radiation from a cellular phone on human sperm motility: an in vitro study", Arch. Med. Res., 37(7), 840 (2006).
3. D. H. Kim, J. H. Ahn, W. M. Choi, H. S. Kim, T. H. Kim, J. Song, Y. Y. Huang, Z. Liu, C. Lu and J. A. Rogers, "Stretchable and foldable silicon integrated circuits", Science, 320(5875), 507 (2008).
4. J.-H. Ahn and J. H. Je, "Stretchable Electronics: Materials, Architectures and Integrations", J. Phys. D: Appl. Phys., 45(10), 103001 (2012).
5. J. A. Rogers, T. Someya and Y. Huang, "Materials and mechanics for stretchable electronics", Science, 327(5973), 1603 (2010).
6. D.-H. Kim and J. A. Rogers, "Stretchable Electronics: Materials Strategies and Devices", Adv. Mater., 20(24), 4887 (2008).
7. D. D. L. Chung, "Materials for Electromagnetic Interference Shielding", J. Mater. Eng. Perform., 9(3), 350 (2000).
8. M. H. Al-Saleh and U. Sundararaj, "Electromagnetic Interference Shielding Mechanisms of CNT/Polymer Composites", Carbon, 47(7), 1738 (2009).
9. G. Hartsgrove, A. Kraszewski and A. Surowiec, "Simulated biological materials for electromagnetic radiation absorption studies", Bioelectromagnetics, 8(1), 29 (1987).
10. S. W. Phang, M. Tadokoro, J. Watanabe and N. Kuramoto, "Synthesis, characterization and microwave absorption property of doped polyaniline nanocomposites containing TiO_2 nanoparticles and carbon nanotubes", Synt. Met., 158(6), 251 (2008).
11. E. Kim, D. Y. Lim, Y. Kang and E. Yoo, "Fabrication of a stretchable electromagnetic interference shielding silver nanoparticle/elastomeric polymer composite", RSC Adv., 6(57), 52250 (2016).

12. S. K. Dhawan, N. Singh and S. Venkatachalam, “Shielding behaviour of conducting polymer-coated fabrics in X-band, W-band and radio frequency range”, Synt. Met., 129(3), 261 (2002).
13. T. Makela, S. Pienimaa, T. Taka, S. Jussila and H. Isotalo, “Thin Polyaniline Films in EMI Shielding”, Synt. Met., 85(1-3), 1335 (1997).
14. Y. Wang and X. Jing, “Intrinsically conducting polymers for electromagnetic interference shielding”, Polym. Adv. Technol., 16(4), 344 (2005).
15. K.-S. Kim, D.-H. Choi and S.-B. Jung, “Overview on Thermal Management Technology for High Power Device Packaging”, J. Microelectron. Packag. Soc., 21(2), 13 (2014).
16. K.-S. Kim, D.-H. Choi and S.-B. Jung, “Overview on Thermal Management Technology for High Power Device Packaging”, J. Microelectron. Packag. Soc., 21(2), 13 (2014).
17. S. Kim and T.-S. Kim, “Adhesion Reliability Enhancement of Silicon/Epoxy/Polyimide Interfaces for Flexible Electronics”, J. Microelectron. Packag. Soc., 19(3), 63 (2012).
18. D.-H. Nam, J.-H. Lee, N.-R. Kim, Y.-Y. Lee, H.-W. Yeon, S.-Y. Lee and Y.-C. Joo, “One-step structure modulation of electrospun metal-loaded carbon nanofibers: Redox reaction controlled calcination”, Carbon, 82, 273 (2015).
19. A. Tuteja, W. Choi, G. H. McKinley, R. E. Cohen and M. F. Rubner, “Design Parameters for Superhydrophobicity and Superoleophobicity”, MRS Bulletin, 33(08), 752 (2011).